International Journal on Magnetic Particle Imaging
Vol 9, No 1, Suppl 1, Article ID 2303010, 4 Pages

Infinite Science Publishing

Proceedings Article

Sparse view sinogram restoration network for improving temporal resolution of projection magnetic particle imaging

Xiangjun Wu[a,b] · Jingying Jiang[a] · Hui Hui[b] · Jie Tian[a,b,*]

[a]School of Engineering Medicine & School of Biological Science and Medical Engineering, Beihang University, Beijing, China
[b]CAS Key Laboratory of Molecular Imaging, Institute of Automation, Chinese Academy of Sciences, Beijing, China
*Corresponding author, email: jie.tian@ia.ac.cn

Abstract

The acquisition views of projection magnetic particle imaging (MPI) limit the temporal resolution of tomographic imaging. When the views of projection are insufficient (sparse view), the streaking artifacts will be introduced after filtered back-projection. The current solutions to the sparse view problem in computed tomography can be divided into three categories, iterative reconstruction, image post-processing, and sparse view sinogram restoration. The first one is computationally intensive and the parameters are difficult to determine. The latter two are data-driven deep learning methods that require large-scale trainable datasets. However, with the data scarcity limitation of MPI, the complex features of the image domain will make the network easy to overfit. Therefore, we propose a sparse view sinogram restoration network for MPI to improve the temporal resolution of tomography. We validate the effectiveness of the proposed method on a simulated dataset and outperform iterative reconstruction and image post-processing methods.

I. Introduction

With its advantages in sensitivity and temporal resolution, MPI has made great progress in biomedical applications, such as, nerve density visualization [1], plaques detection [2], and stem cell monitoring [3].

Currently, the scanning modes of MPI are mainly divided into two categories, field free point and field free line, the latter has higher sensitivity and temporal resolution [4]. However, tomographic reconstruction using FFL scans requires a full and dense view of 2D projections, which also limits its temporal resolution. Therefore, the concept of sparse view reconstruction can be introduced, which improves imaging resolution by reducing the number of projection acquisitions and has been extensively studied in CT. The current mainstream methods can be divided into three categories: (1) iterative reconstruction methods [5], (2) image post-processing methods [6], and (3) sparse view sinogram restoration methods [7]. The iterative reconstruction method has the limitations of large amount of calculation and difficult to determine parameters. The latter two are data-driven deep learning methods that require large amounts of training data. For image post-processing methods, since the features of the image domain are more complex, the risk of network overfitting will be increased, and the post-processing method cannot perfectly remove streaking artifacts. Therefore, we propose a sinogram restoration

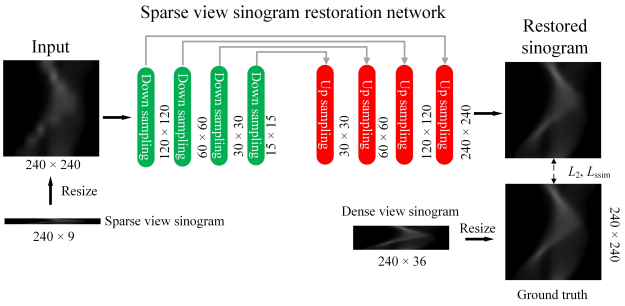

Figure 1: Structure of sparse view sinogram restoration network. Since the sparse sinogram network contains four down-sampling modules, we resize the original image to 240 x 240 (realized through bilinear interpolation in OpenCV).

network to deal with the issue of sparse view reconstruction in projection MPI.

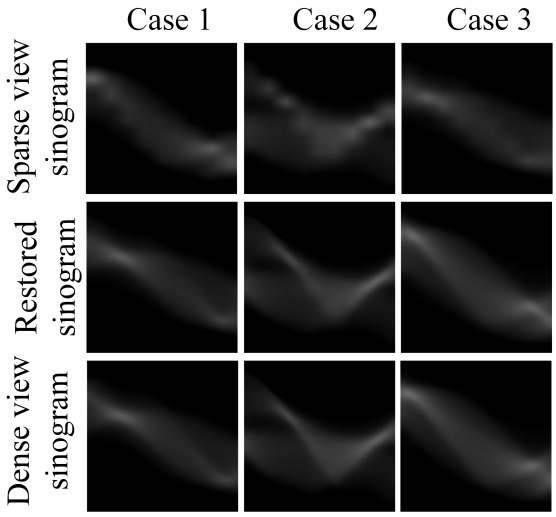

Figure 2: Results of sparse view sinogram restoration.

II. Material and methods

A large amount of data is often required to train deep neural networks, however, the cost of obtaining large-scale real MPI data is enormous. A common practice is to generate MPI simulation datasets to train deep neural networks. Therefore, we also adopt this strategy, we simulate the scanning modes of projection MPI, and simulate 2400 tomographic slices, of which 2000 are used for training and 400 are used for validation. For each slice, we perform dense view (acquisition range π, acquisition interval 5 °) and sparse view (acquisition range π, acquisition interval 20°) projection to obtain the corresponding sinograms.

The sparse view sinogram recovery network adopts the structure of UNet [8] (showed in Fig. 1), which including four down sampling (including two convolutional and a pooling layers) and up sampling blocks (including two convolutional and a up sampling layers). The input and ground truth (GT) of the network correspond to the resized sparse view sinogram (S^{sv}) and the dense view sinogram (S^{dv}). The loss function used in network training consists of two parts, L_2 loss and structural similarity (SSIM) loss L_{ssim}. The L_2 loss is used to calculate the pixel distance between the sinogram restoration results of network ($S^{restore}$) and GT, and can be defined as:

$$L_2 = \sum_{i}^{n}\sum_{j}^{m}\left(S_{i,j}^{restore} - S_{i,j}^{dv}\right)^2 . \quad (1)$$

where the m and n represent the height and width of the image, respectively. And the L_{ssim} can be defined as:

$$L_{ssim} = 1 - SSIM(S^{restore} - S^{dv}) . \quad (2)$$

Therefore, the final loss can be expressed as:

$$L_{all} = L_2 + \mu L_{ssim} . \quad (3)$$

since the scales of the L_2 and L_{ssim} are different, L_2 is much larger than L_{ssim}, where L_2 controls the pixel-level distance, and L_{ssim} controls the overall structural similarity of the image. Through the adjustment of hyper-parameters μ, the network can learn the characteristics of sinogram in pixel details and overall structure. The hyperparameters μ are determined by selecting the optimal parameters in the internal validation set by grid search.

The SSIM, peak signal to noise ratio (PSNR), and mean square error are used to evaluate the performance of sparse view sinogram restoration.

III. Results and discussion

III.I. Results of sparse view sinogram restoration

The quality of sparse view sinogram restoration directly affects the results of tomographic reconstruction, and we first evaluate the sparse view sinogram restoration results of the network. The results of sinogram recovery are shown in Fig 2.

There exists quite difference on the features of the simulated imaging targets in the image domain, however, the feature distributions in the projection domain are similar, which is also more conducive to the learning of the network. Therefore, the restoration results of the sparse view sinogram are very close to the dense view sinogram.

The quantitative results are presented in Table 1. The SSIM of the sinogram restoration results is greater than 0.95 and the PSNR is greater than 35, which further illustrates the good performance of the sparse view sinogram restoration network.

10.18416/ijmpi.2023.2303010

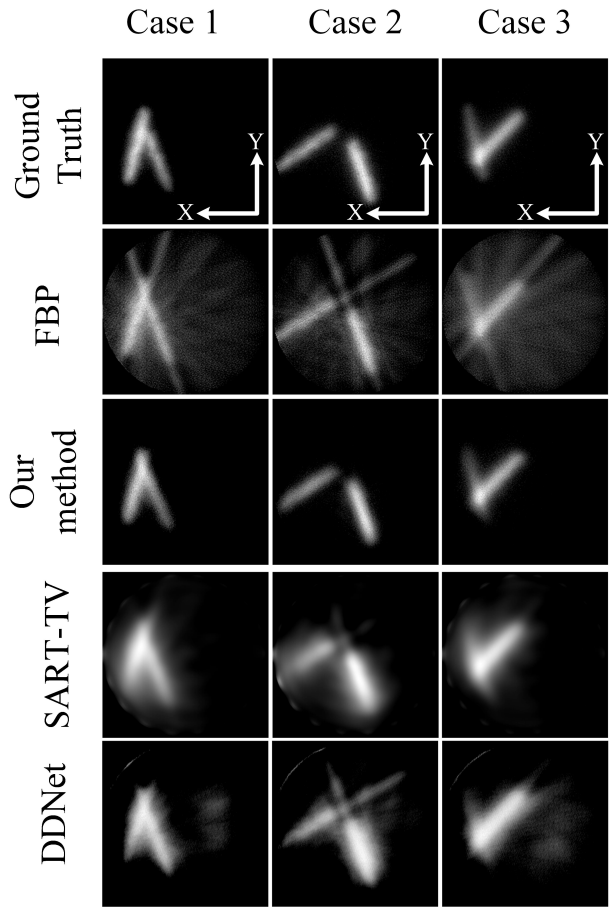

Figure 3: Results of tomography reconstruction.

Table 1: Performance of sparse view sinogram restoration.

	SSIM	PSNR	MSE
Restored sinogram	0.978	38.596	13.637

III.II. Results of tomography reconstruction

The purpose of sparse view sinogram restoration is to complement the projections of the unacquired angles, thus avoiding the generation of streaking artifacts in the tomographic reconstruction. Therefore, we perform the filtered back-projection reconstruction of the sinogram restoration results obtained in the previous section to obtain tomographic slices. And we compare the iterative reconstruction (SART-TV [5]) and image post-processing (DDNet [6]) methods. The results are shown in Fig. 3 and Table 2, respectively.

Since MPI has no background structure information, the number of projections required for its reconstruction is much smaller than that of CT. For sparse view reconstruction in MPI, only 9 views of projections are used for tomographic reconstruction. Therefore, in this case, the results of iterative reconstruction are not satisfactory. For image post-processing networks, due to the more complex features of the image domain, excessive learning increases the risk of network overfitting and poor artifact removal in and around the signal. Our proposed sparse view sinogram restoration network avoids the generation of streaking artifacts and achieves the best performance.

Table 2: Performance of tomography reconstruction

	SSIM	PSNR	MSE
SART-TV	0.328	15.852	1752.913
DDNet	0.792	21.053	615.589
Ours	0.801	31.485	65.790

IV. Conclusion

In this study, we propose a sparse-view sinogram restoration network that improves the tomographic temporal resolution of projection MPI by four times. The effectiveness of the proposed method has been preliminarily validated on simulated datasets and outperforms iterative reconstruction and deep learning-based image post-processing methods.

Acknowledgments

This work was supported in part by the National Key Research and Development Program of China, Grant 2017YFA0700401; the National Natural Science Foundation of China, Nos. 62027901, 81827808, 81971662, 81227901; the CAS Youth Innovation Promotion Association, Grant 2018167 and CAS Key Technology Talent Program; Natural Science Foundation of Beijing City, 7202105; Beijing Natural Science Foundation, JQ22023; The Project of High-Level Talents Team Introduction in Zhuhai City, Zhuhai HLHPTP201703; Guangdong Key Research and Development Program of China, 2021B0101420005. The authors would like to acknowledge the instrumental and technical support of Multimodal Biomedical Imaging Experimental Platform, Institute of Automation, Chinese Academy of Sciences.

Author's statement

Authors state no conflict of interest. Informed consent has been obtained from all individuals included in this study. Conflict of interest: Authors state no conflict of interest. Informed consent: Not applicable. Ethical approval: Not applicable.

References

[1] H. You, W. Shang, X. Min, J. Weinreb, Q. Li, M. Leapman, L. Wang, and J. Tian, "Sight and switch off: Nerve density visualization for interventions targeting nerves in prostate cancer," Sci. Adv., vol. 6, no. 6, p. eaax6040, 2020.

[2] W. Tong, H. Hui, W. Shang, Y. Zhang, F. Tian, Q. Ma, X. Yang, J. Tian, and Y. Chen, "Highly sensitive magnetic particle imaging of vulnerable atherosclerotic plaque with active myeloperoxidase-targeted nanoparticles," Theranostics, vol. 11, no. 2, p. 506, 2021.

[3] Q. Wang, X. Ma, H. Liao, Z. Liang, F. Li, J. Tian, and D. Ling, "Artificially engineered cubic iron oxide nanoparticle as a high-performance magnetic particle imaging tracer for stem cell tracking," ACS Nano, vol. 14, no. 2, pp. 2053–2062, 2020.

[4] J. J. Konkle, P. W. Goodwill, O. M. Carrasco-Zevallos, and S. M. Conolly, "Projection reconstruction magnetic particle imaging," IEEE Trans. Med. Imaging, vol. 32, no. 2, pp. 338–347, 2012.

[5] H. Yu and G. Wang, "Compressed sensing based interior tomography," Phys. Med. Biol., vol. 54, no. 9, p. 2791, 2009.

[6] Z. Zhang, X. Liang, X. Dong, Y. Xie, and G. Cao, "A sparse-view CT reconstruction method based on combination of DenseNet and deconvolution," IEEE Trans. Med. Imaging, vol. 37, no. 6, pp. 1407–1417, 2018.

[7] H. Lee, J. Lee, H. Kim, B. Cho, and S. Cho, "Deep-neural-network-based sinogram synthesis for sparse-view CT image reconstruction," IEEE Trans. Radiat. Plasma Med. Sci., vol. 3, no. 2, pp. 109–119, 2018.

[8] O. Ronneberger, P. Fischer, and T. Brox, "U-net: Convolutional networks for biomedical image segmentation," in International Conference on Medical image computing and computer-assisted intervention, 2015, pp. 234–241.

10.18416/ijmpi.2023.2303010